

Preliminary Assessment of Performance and Cost of a Cubesat Component of the Earth Science Decadal Survey

Daniel Selva
Massachusetts Institute of Technology
77 Massachusetts Ave Cambridge, MA 02139; +1 617 682 6521
dselva@mit.edu

David Krejci
Vienna University of Technology
Karlsplatz 13, Vienna 1040, Austria; +43 1 588010
david.krejci.fl@fotec.at

ABSTRACT

In 2007, The National Research Council released a report known as the Earth Science Decadal Survey. This report lays out an architecture for a holistic Earth Observation Program consisting of 17 missions to be flown in a decade for a total cost of about \$7B. Six years after, mission cost estimates have grown by 70% on average, and at the current levels of funding for NASA Earth Science, it would take about 40 years to fly these missions. Furthermore, missions that played central roles in satisfying the needs of the Earth science community have not materialized, due to launch failures, mission cancellations, severe delays or descoping processes. The Earth Science community is in desperate need of novel architectures for Earth observation missions that can satisfy at least part of the scientific requirements at a fraction of the cost of the Decadal Survey missions. Cubesats have the potential to become an important component of such novel architectures by providing low-cost opportunities to fly advanced miniature instruments such as GNSS receivers in radio occultation and reflectometry modes, visible and near-infrared imagers, short-wave infrared spectrometers, millimeter-wave radiometers, microbolometers, and so forth.

While Cubesats have hitherto mostly been used for technological demonstration and educational purposes, there has been some emphasis lately in developing Cubesats capable of satisfying demanding scientific requirements. In a recent paper, a survey and assessment of the capabilities of Cubesats as a platform for Earth observation instruments of high scientific value, was presented. This paper takes that work a step further by analyzing, in terms of both performance and cost, several constellations of Cubesats carrying such instruments. The performance of an architecture (i.e., a certain mix of constellations of Cubesats) is computed by assessing its potential to satisfy the Decadal Survey scientific requirements. This is done leveraging prior work on the development of a rule-based expert system for assessing the relative merit of Earth observing system architectures.

Different constellation designs carrying different mixes of payloads are analyzed using performance and cost models. Non-dominated architectures in the Pareto sense are identified, and one preferred architecture is analyzed in more detail. A preliminary mission analysis is conducted for this preferred architecture, and its cost-effectiveness is compared to that of the original Decadal Survey architecture.

The paper shows how, while Cubesats still suffer from serious limitations in terms of their performance and capabilities for Earth science, they are a very cost-effective way of satisfying a relatively large portion of the Decadal Survey requirements.

NOMENCLATURE

archs	Architectures	GRAV	Gravity instrument (accelerometer)
cdf	Cumulative distribution function	IMAG	Imager instrument
ERB	Earth radiation budget instrument	IR	Infrared
FOV	Field of view	ISS	International space station
FY	Fiscal year	LW	Longwave
GNSS	Global navigation satellite system	MMAS	Millimeter-wave atmospheric sounder
GPS	Global positioning system	ninstr	Number of instruments
GPS-R	GPS in reflectometry mode	norb	Number of orbits
GPS-RO	GPS in radio occultation mode	nvars	Number of variables
		NREC	Non-recurring cost

REC	Recurring cost
SPEC	Spectrometer
SSO	Sun-synchronous orbit
SW	Shortwave
STK	Satellite Tool Kit (AGI)
TEC	Total electron content
UV	Ultraviolet
VNIR	Visible and near-infrared

INTRODUCTION

In 2004, The National Research Council was requested to conduct a study to generate recommendations in terms of space-based observations of the Earth's surface and atmosphere. The goal of the study was to reach consensus and suggest a set of missions that would satisfy the needs of all disciplines of the Earth sciences for the next decade. Three years after, the Earth Science Decadal Survey report was released. The Decadal Survey proposed an architecture consisting of 17 missions to be flown in a decade for a total cost of about \$7B¹.

However, in 2013, none of the missions proposed have actually been launched, and it is very likely that only one or 2 missions will be launched before 2015, a nd perhaps 3 or 4 before 2020. Mission cost estimates have grown by 70% on average, and at the current levels of funding for NASA Earth Science, it will take about 40 years to fly these missions². Furthermore, missions that played central roles in satisfying the needs of the Earth science community have not materialized: Glory and OCO were lost at launch, NPOESS/JPSS has suffered severe delays and descopeing processes, GPM has been delayed, and recently, the CLARREO and DESDYNI missions have been cancelled.

The Earth Science community is in desperate need of novel architectures for Earth observation missions that can satisfy at least part of the scientific requirements at a fraction of the cost of the Decadal Survey missions. Cubesats have the potential to become an important component of such novel architectures by providing low-cost opportunities to fly advanced miniature instruments such as GNSS receivers in radio occultation and reflectometry modes, visible and near-infrared imagers, short-wave infrared spectrometers, millimeter-wave radiometers, bolometers, and so forth.

While Cubesats have hitherto mostly been used for technological demonstration and educational purposes, there has been some emphasis lately in developing Cubesats capable of satisfying demanding scientific requirements. In a recent paper, a survey and assessment of the capabilities of Cubesats for Earth observation was presented³. This paper identified

several opportunities for high science-output Cubesat-based missions in different fields of the Earth sciences, including ocean biology, Earth radiation budget, weather prediction, and land ecosystems.

This paper takes that work a step further by conducting a preliminary analysis of performance and cost for a very large number of constellations of Cubesats carrying such instruments.

The performance of an architecture (i.e., a certain mix of constellations of Cubesats) is computed by assessing its potential to satisfy the Decadal Survey scientific requirements. This is done leveraging prior work on the development of a rule-based expert system for assessing the relative merit of Earth observing system architectures⁴. The expert system compares the capabilities of a constellation with a large database of requirements from different disciplines under a variety of attributes (e.g., spatial resolution, temporal resolution, and accuracy).

The cost estimate of an architecture includes rough estimates for payload cost, bus cost, and launch cost. Separate estimates are provided for recurring and non-recurring costs, which are then added assuming a lifetime of ten years and no discount rate.

The architectural tradespace is defined by all possible assignments in a bipartite graph of orbits and instruments. In other words, given a number of candidate orbits and candidate instruments, an architecture is defined by an assignment of instruments to orbits, where each instrument can be assigned to any number of orbits – including all of them, or none of them. Orbits without instruments are also allowed.

Since the full architectural tradespace is extremely large for relatively small numbers of instruments and orbits, a multi-objective genetic algorithm is used to explore the cost-performance space. The genetic algorithm provides an approximation to the true cost-performance Pareto frontier. Architectures in this approximate Pareto front are identified and analyzed, by looking at their sensitivity to uncertainties in some of the model parameters.

One preferred architecture that appears as a good compromise of cost and performance under a wide variety of scenarios is analyzed in more detail. A preliminary mission analysis is conducted for this preferred architecture, and its cost-effectiveness is compared to that of the original Decadal Survey architecture.

The paper shows how, while Cubesats still suffer from serious limitations in terms of their performance and

capabilities for Earth science, they are a very cost-effective way of satisfying a portion of the Decadal Survey requirements. This would increase the funding available at NASA to fund more sophisticated missions that can satisfy stringent scientific requirements. In other words, this paper suggests that, much like NASA transitions weather missions to NOAA when they are considered mature enough to be operational, NASA and other organizations should consider transitioning to the commercial sector – represented here by the Cubesat paradigm – for the growing subset of measurements that are compatible with the state of the art of Cubesat technology.

METHODS

Overview

The goal of this project is to explore the tradespace of architectures that result from assigning different subsets of instruments to different orbits, in the science-cost space. The methodology consists of six steps and is summarized in Table 1. The first step is to identify and characterize a set of candidate instruments and orbits. This was done leveraging using publicly available information from different sources, especially from the GEOScan program⁵. The second step is to pre-compute the capabilities of all instrument subsets under each orbit, taking into account synergies between the instruments in the same orbit. These capabilities are essentially the measurements that each instrument can take and the data products that can be generated with those measurements. This pre-computation allows for a much faster evaluation in the third step, which is the tradespace exploration using a multi-objective genetic algorithm. The fourth step is to analyze the results provided by the genetic algorithm in order to facilitate the selection of one architecture (fifth step). Finally, a preliminary mission analysis is conducted on the selected architecture using AGI's STK software.

Candidate instrument characterization

Recently, Selva and Krejci³ analyzed the capabilities of Cubesats for Earth observation. This study assessed instrument capabilities regarding anticipated measurement utility, scientific readiness of the measurement and technology readiness of the Cubesat bus required. One of the outcomes of the paper was a shortlist of instruments that would potentially provide high scientific output at a fraction of the cost of a large-scale Earth observing program by leveraging the Cubesat standard. These instruments are the following: a GNSS receiver in radio occultation mode; a GNSS receiver in reflectometry mode; a microbolometer for Earth radiation budget measurements; a VNIR spectrometer for ocean color and vegetation

measurements; and a VNIR imager. On a similar note, Dyrud et al published a paper describing the GEOScan program, where it is proposed to fly some of the same instruments as hosted payloads in the Iridium NEXT constellation⁶. The potential characteristics of such instruments are discussed below and summarized in Table 1. The GEOScan assumptions for some of these instruments were often taken as baseline.

GNSS receiver in radio occultation mode—The GNSS receiver in radio occultation mode (GPS-RO) measures the difference in Doppler shift between two GPS signals: one received from a reference, non-occluding GPS satellite, and one received from an occulting GPS satellite. This difference in Doppler shift comes from the difference in path length of the atmosphere that the two waves traverse. Knowing the real positions of the two GPS satellites and the GPS receiver, it is possible to infer a bending angle of the signal coming from the occulting GPS, and therefore the refractivity of the atmosphere. From refractivity, one can infer several atmospheric parameters, namely total electron content (TEC), temperature or pressure, and humidity. The CanX-2 Cubesat flew a GPS-RO experiment carrying a single low-gain antenna for both positioning and occultation, and reported errors below 10^{11} electrons/m³⁷. The GEOScan project based on a COTS receiver reported 300 soundings per day per sensor and an error < 3 TEC units (i.e., $3 \cdot 10^{16}$ electrons/m²)⁶. Note that the sensitivity of the GPS-RO to measure atmospheric profiles is limited to the upper troposphere and stratosphere, where concentration of water vapor is limited.

Microbolometer—The goal of the microbolometer (ERB) is to provide Earth radiation budget measurements of both outgoing SW and LW radiation. Dyrud et al describe a microbolometer for the GEOScan constellation that can measure both total radiation (SW+LW, 0.2-200 μ m) and SW radiation (0.2 to 5 μ m) with an accuracy better than 0.5W/m². It has a wide field-of-view of 124deg to cover the entire Earth's surface, and it has an on-orbit calibration capability.

Millimeter wave sounder—The goal of the passive mm-wave sounder (MMAS) is to measure profiles of atmospheric temperature and pressure through hyperspectral sampling of O₂'s rotational line at 118GHz, and to measure profiles of atmospheric water vapor, humidity, cloud liquid water, and precipitation, through hyperspectral sampling of H₂O's rotational line at 183GHz. Dr Blackwell's instrument⁸ on the Micromas satellite reports an absolute accuracy for atmospheric humidity of 20-30%, and for atmospheric temperature of about 1K. The Micromas sounder weighs about 500g and it has a FOV of 50 deg⁹.

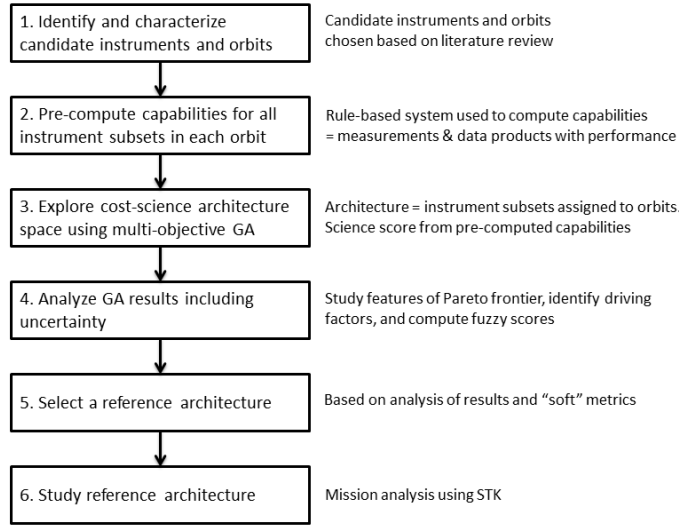


Figure 1: Methodology used in this research project

Table 1: Candidate instrument characteristics

Instrument	GPS-RO ^{10,11}	GPS-R ¹²	ERB ⁶	MMAS ⁸	SPEC ¹³	IMAG ⁶	GRAV ⁶
Mass (g)	200	4900	600	1200	300	300	200
Avg./Peak Power (W)	1.5/1.7	6.0/10	0.3/5.0	2.0/6.0	0.9/1.3	0.6/0.6	1.3
Avg. data rate (kbps)	2.0	100	1.0	20	3.3	4.2	0.7
Dimensions (cm)	8.0x13x1.3	10x10x30	10x9.0x10	10x10x10	3.9x9.8x11	10x10x10	3.8x3.8x3.8
Non-recurring cost (\$M)	0.0	30	1.0	1.0	0.0	1.0	8.0
Recurring cost (\$M)	0.085	0.50	0.11	0.10	0.06	0.1	0.1
Measurement 1	Atmospheric refractivity	Sea surface height	Total LW radiance	Atmospheric humidity	Ocean color	Land use	Geoid and gravity field
Measurement 2	Ionosphere total electrons	Sea surface wind speed	Total SW radiance	Cloud liquid water	Vegetation state	Landcover status	Ocean mass distribution
Measurement 3	Atmospheric humidity	Land surface topography		Precipitation rate	Aerosol optical depth	Cloud mask	Glacier mass distribution
Measurement 4	Atmospheric temperature	Vegetation structure		Hurricane tracking		Disaster monitoring	Groundwater storage
Measurement 5	Atmospheric pressure	Sea ice cover					Seafloor topography
Measurement 6		Snow cover					
Measurement 7		Soil moisture					

Table 2: Synergies between instruments

Instrument1	Instrument2	Synergistic data product	Justification
GPS-RO	GRAV	Gravity field measurements	All useful gravity products are obtained through the combination of non-gravitational accelerations from the accelerometer and precise orbit determination from the GPS receiver.
IMAG	SPEC	Cloud-free land, ocean, and atmospheric images	The cloud mask product of the imager is used to improve the quality of all other ocean color, vegetation, and atmospheric chemistry products
IMAG	MMAS	Cloud-free atmospheric images	The cloud mask product of the imager is used to improve the quality of all other ocean color, vegetation, and atmospheric chemistry products

VNIR spectrometer—The primary goal of the spectrometer (SPEC) is to provide measurements of vegetation state and ocean color. Secondary goals include atmospheric chemistry applications. Minelli et al¹³, Kitts et al¹⁴, Bramall et al¹⁵, and Dyrud et al⁶ describe a space-proven Czerny-Turner spectrometer that covers the spectral range between 200nm-2000nm with a spectral resolution of 0.5nm (although this does not necessarily mean full sampling at this resolution). Two main potential limitations of the spectrometer are its signal-to-noise ratio and the trade-off between imaging capability and spectral sampling. Should the signal-to-noise ratio, spectral sampling, and imaging capability be sufficient, such an instrument would be able to make extremely valuable measurements in the UV (e.g., O₃, NO_x, SO₂) and NIR (e.g., CO, CO₂, CH₄, aerosols). Furthermore, if the instrument had enough imaging capability, the 0.7 μ m water vapor spectral feature could be used to produce water vapor and water vapor transport images. However, these capabilities are not considered in this paper.

VNIR imager— The main goal of the visible imager (IMAG) is to provide multi-purpose 4km-resolution land and ocean imagery for real-time applications such as disaster management. There are several instruments that could be used as the VNIR imager. We base our design on JHU/APL’s MicroCam⁶, which is a 1024 x 1024 15- μ m pixel CMOS camera, configurable with different filters in the 400nm-1000nm spectral range. It weighs about 150g, consumes around 550mW on average, and provides up to 10 frames per second with 10 bits of radiometric resolution. The actual configuration on a 2U Cubesat bus could include 2 of these cameras, one of which would carry a 0.76 μ m filter for cloud mask.

Gravity sensor—The gravity sensor (GRAV) is an accelerometer that will provide non-gravitational accelerations (i.e., the result of forces such as drag). Draper Laboratory has developed a 3-axis MEMS accelerometer that has a sensitivity of 100 ng/ $\sqrt{\text{Hz}}$ or better in the 0.0001-0.001Hz band¹⁶. In combination with GPS information providing precise relative position and velocity of the spacecraft, one can infer the accelerations purely due to gravity and thus the Earth’s gravity field. The synergistic combination of the GPS receiver and the accelerometers is capable of providing information about the Earth’s gravity field, from which information concerning glacier mass balance and ocean mass distributions can be obtained.

Candidate orbits

Orbit selection is extremely important in Earth observation missions because it affects both the science and the cost of the mission. For this analysis, four orbits

were chosen as candidates based on both performance and cost considerations. These orbits are listed in Table 3 in descending order of launch cost. All orbits are LEO circular orbits.

Table 3: List of candidate orbits

Altitude	Inclination	Launch cost
600km	SSO (97.8deg)	\$10M \pm 50%
600km	ISS (51.6deg)	\$8M \pm 50%
400km	Polar (90 deg)	\$6M \pm 50%
400km	Tropical (28.5deg)	\$3M \pm 50%

We considered two altitudes: 600km and 400km. The 600km orbit is a good compromise between lifetime and coverage. The 400km orbit has lower lifetime due to atmospheric drag and degraded coverage, but has lower launch cost, better spatial resolution, and increased sensitivity to the Earth’s gravity and magnetic fields.

As for inclinations, we considered four different inclinations: two driven by science requirements, namely 97.8deg (sun-synchronous at 600km), 90 deg (true polar), 51.6 deg (the inclination of the ISS), and 28.5 deg (tropical). Many applications require SSO orbits in order to guarantee similar illumination conditions across measurements. SSO have almost global coverage with potentially reduced coverage in the poles. True polar orbits do not guarantee similar illumination conditions, but offer a better coverage of the polar regions, and therefore they are preferred in some disciplines in which the poles are regions of interest, such as cryospheric or solid Earth studies. The ISS inclination allows some reduction in launch cost, since ISS resupply mission can be leveraged. This mid-latitude inclination is also a relatively good choice for some applications that require good diurnal sampling (e.g., oceanography to avoid tidal aliasing). Finally, the tropical inclination provides optimal coverage of the tropical region, which is very important in some applications including weather forecasting and hurricane tracking amongst others. Furthermore, it has advantages in launch cost with respect to the SSO and polar, as 28.5deg is the latitude of Cape Canaveral, and therefore injection into this orbit from Cape Canaveral does not require an expensive change of inclination.

Synergies between instruments

The capabilities of a certain instrument subset are not a plain superposition of the capabilities of the individual instruments, due to the presence of synergies between instruments. Synergies between two or more instruments appear when measurements taken by individual instruments are combined to create a new measurement that is different from the individual

measurements in one or more attributes (e.g., spatial resolution, temporal resolution). For example, in a typical altimetry mission, the radar altimeter is flown with a microwave radiometer for atmospheric correction, and with some orbitography instrument (e.g. GPS, DORIS receiver) for precise orbit determination. The altimetry products that can be generated with this instrument subset are of much better quality than those that could be generated with the radar only. Synergies are captured in the form of logical rules. Generally, synergy rules are important in the science evaluation process because the new measurement can and usually does satisfy more requirements than the individual measurements.

Table 2 contains the synergies between the instrument set modeled in the expert system. Namely, two major synergies are modeled: 1) combination of GPS and accelerometer measurements to produce gravity data products; 2) combination of cloud mask data from the imager with several other products to obtain cloud-free datasets. Note that there might be several other synergies between these instruments that do not affect the satisfaction of Decadal Survey requirements.

Rule-based science merit evaluator

The model used to compare architectures in their ability to satisfy Decadal Survey requirements is based on previous work developed during Dr Selva’s doctoral dissertation⁴.

The model uses a rule-based expert system to systematically compare the capabilities of different system architectures (i.e., the measurements and data products that it can generate as a system) with a set of measurement requirements. These measurement requirements are logical rules that express the needs in terms of spatial resolution, temporal resolution, accuracy and so forth for different data products spanning all disciplines of the Earth sciences.

For each attribute or combination of attributes, a preference function is specified that transforms a numerical value in physical units (e.g. 1.5km of vertical spatial resolution) or a fuzzy value (e.g., “High”, “Low”) into an adimensional satisfaction value (e.g., 75%). In most cases, these preference functions take the form of a multi-step function with a target value and a threshold value. Any attribute with a value beyond the target gets 100% satisfaction; values between the target and the threshold value get 50% of satisfaction; finally, any value below the threshold gets 0% satisfaction. An example is given in Table 4 for atmospheric temperature. Note that, in some cases, more than 2 levels are used to model the preference function.

Table 4: Example of requirement rules for atmospheric temperature data products

Attribute	Target	Threshold
Vertical Spatial resolution	1km	2km
Horizontal Spatial Resolution	5km	10km
Temporal Resolution	0.5h	1h
Accuracy (mean)	1K	2K
All-weather capability	Yes	Yes

Satisfaction at the attribute level is combined at the measurement level using other rules which contain weighted averages and logical operators. The aggregation rule by default multiplies the attribute satisfactions to produce a measurement satisfaction. Finally, satisfaction of different scientific communities is computed as a function of the satisfaction of their measurement requirements, and an overall value of the architecture is calculated as a weighted average of the satisfaction of the different scientific communities.

While it is certainly not easy to quantify scientific value in absolute terms, this metric intends to be a rigorous means for relative comparison of architectures in their ability to satisfy Decadal Survey requirements. A more in-depth discussion of the science performance model is provided in Selva and Crawley¹⁷.

Fuzzy science scores

As recognized in Selva’s thesis, there are a variety of sources of uncertainty in these relative scientific merit scores. First of all, it is hard to assess scientific value because of the nature of science itself. Some scientific discoveries may lead to new applications or even completely new fields. Predicting these cases is obviously impossible. Furthermore, some of the instruments being assessed may not be fully developed yet, and therefore there is some uncertainty in their capabilities and performance. And even for a fully developed instrument, scientists may disagree as to what their ability to satisfy a certain requirement is, or even worse, they might disagree on what the requirement should be altogether.

We fully acknowledge these uncertainties, and in order to at least attempt to capture them, we use the notion of fuzzy science scores. Fuzzy science scores provide fuzzy assessments of how well requirements are satisfied. Namely, a requirement can have five levels of satisfaction: Full, Most, Half, Some, and Marginal. These fuzzy assessments are associated to the membership functions shown in Table 5. In this work, simple interval analysis was used to propagate the uncertainty, although more sophisticated methods using Zadeh’s fuzzy sets¹⁸ are also available in the tool.

Table 5: Correspondence between fuzzy requirement scores and numerical intervals

Fuzzy value	Interval
Full	[1.0; 1.0]
Most	[0.66; 1.0]
Half	[0.4; 0.6]
Some	[0.33; 0.5]
Marginal	[0.0; 0.33]

Cost estimation

Estimating the lifecycle cost of a space mission is challenging for several reasons, including the relatively small number of satellite missions of any given type developed so far, and the large uncertainty on several mission aspects such as technology maturity. Estimating the cost of a Cubesat mission has additional challenges because most of the missions have been developed by universities, where keeping track of labor cost is extremely hard. Limited cost data on specific Cubesat missions is available in Refs¹⁹⁻²².

The cost model used to compare architectures in this work is very simple and contains estimates of non-recurring and recurring payload cost, non-recurring and recurring bus cost, launch cost, and non-recurring and recurring operations cost. The model provides both an expected value and an error bar to produce a “fuzzy cost”.

The parameters used in the cost model are summarized in Table 6. All values are in FY13\$M. Estimates for non-recurring and recurring payload costs are provided in Table 1. A standard deviation of 20% was used for all instruments. Non-recurring payload costs are added once for each instrument that is present in the architecture. No learning curves are assumed.

Bus costs are estimated per kg of bus, assuming 1.0 FY13\$M per kg (i.e., approximately per Cubesat unit) for non-recurring costs, and 0.2 FY13\$M per kg for recurring costs. Hence, bus costs are three times larger for a 3U Cubesat than for a 1U Cubesat.

Launch costs are computed assuming one launch per orbital plane and using the information provided in Table 3.

Finally, 1.0 FY13\$M is added to account for non-recurring costs for developing the ground segment, and 0.1 FY13\$M per kg are added per year for operating the ground station. Note that non-recurring ground station costs are added once to all architectures regardless of the number of instruments, including the “empty” architecture containing no instruments at all.

Table 6: Cost model parameters. NREC = non-recurring cost. REC = recurring-cost

Parameter	Value
NREC ground cost	\$1.0M ± 50%
NREC instrument cost	(See Table 1)
NREC bus cost	\$1.0M ± 20%
REC instrument cost	(See Table 1)
REC bus cost	\$0.2M ± 20%
REC operations cost per year	\$0.1M ± 50%
REC launch cost	(See Table 3)

Tradespace exploration

The tradespace exploration problem is formulated as a combinatorial optimization problem, namely an assignment problem. Let $I = \{I_1, I_2, \dots, I_n\}$ be the set of candidate instruments defined in the previous section, and let $O = \{O_1, O_2, \dots, O_m\}$ be the set of candidate orbits defined in Table 3. Then an architecture is defined as an assignment of instruments to orbits. Such assignment can be represented for example by means of a binary matrix A , where its element $A_{ij}=1$ if instrument I is assigned to orbit j , and $A_{ij}=0$ otherwise. Since no constraints are imposed on the sums of the rows and columns of A , the size of the architectural tradespace is simply given by 2^{nm} . For 7 instruments and 4 orbits, this is equal to $2^{28} \approx 268$ million architectures.

The metrics of interest are cost and performance, as defined in the previous section. While the cost model is very cheap computationally, the performance model takes on the order of a few seconds to run for a single architecture. This long time is mostly driven by the synergies between instruments that recursively create new data products that need to be matched against the requirements. Since synergies are mostly established between instruments in the same orbit, performance and cost of every subset of instruments in each orbit could in theory be precomputed off-line and stored in a hashmap. However, there might be redundancies between instruments on different orbits, as two instruments may satisfy the same measurement requirements. In order to avoid double-counting redundant capabilities, the hashmap actually contains the capabilities – instead of the score- of each subset of instruments in each orbit. Then, the value of an architecture can readily be obtained by retrieving the capabilities from the instrument subsets in each orbit, and computing the score based on the combined capabilities.

This process allows for important time savings in the performance function evaluation. However, this reduction still does not allow for full factorial evaluation of the tradespace on a standard computer.

The use of an exact combinatorial optimization algorithm such as any variation of linear programming, cutting planes, or dynamic programming is also impossible due to the interactions between the instruments (synergies, redundancies).

Therefore, Matlab’s variant of NSGA-II, a controlled elitist multiobjective genetic algorithm was used to explore the resulting two-objective space²³. Architectures were encoded in a bit string genome of length $n_{instr} \cdot n_{orb} = 28$. Cost and performance, normalized so that they lie in the range 0-1, were used for the calculation of the Pareto rankings, with no equality, inequality, or non-linear constraints. The rest of settings for the genetic algorithm are shown in Table 7.

Table 7: Settings for the multiobjective genetic algorithm

Parameter	Value
Population size	4 subpopulations of $4 \cdot n_{vars} = 112$ archs (total 448 archs)
Initial population	Random
Distance measure function	Distance crowding on genotype
Pareto fraction	0.35
Function tolerance	0.001
Stall generation limit	150
Mutation function	Bitwise mutation
Crossover function	Single-point crossover
Selection function	Tournament selection
Migration fraction	0.2
Migration direction	Forward

Mission analysis

AGI’s Satellite Tool Kit (STK) software was used for more detailed mission analysis of the selected Cubesat constellation. The architecture was loaded in the scenario as a constellation, and propagated for 7 days with a time step of 60s, using the High Precision Propagator, which takes into account both the J2 effect and atmospheric drag. A coverage grid from -90 to 90 deg latitude was defined, with a granularity of 6deg in latitude and longitude. Furthermore, one ground station was added using the coordinates of Boston, MA for access calculations.

Given this scenario, the distribution of revisit times was computed for each point in a coverage grid throughout the simulation, using the entire constellation of sensors (with their fields of view adequately modeled) as the only assets. Furthermore, for each Cubesat, the percentage of sunlight time and the accesses to the ground station were computed. Note that the revisit

times computed in this fashion are only relevant to some of the instruments, and therefore we will only report a single number for the constellation instead of providing different numbers for each individual instrument.

RESULTS

Tradespace exploration

This section presents the results of the tradespace exploration using the multiobjective genetic algorithm. Tens of thousands of architectures were analyzed in terms of science and cost. Science scores ranged between 0 for the “empty architecture” (no instruments selected) and 0.175 for the “full architecture” (all instruments assigned to all orbits). Note that all orbits are required to achieve the highest score orbit. Architectures that are missing one or more orbits cannot achieve the highest science score, because the value provided through the GPS radio occultation instrument increases with the number of soundings, and thus with the number of instruments and orbits.

Cost estimates ranged between \$1M for the empty architecture (the cost of developing the ground station) and \$104M. This loosely means that the “full architecture” is capable of satisfying ~18% of the Decadal objectives for ~\$100M, that is, around 1% of an optimistic \$10B cost estimate for the entire Decadal. In other words, this suggests that this Cubesat constellation could potentially be 5 to 10 times more cost efficient than any of the Decadal missions.

Pareto Frontier—The approximate Pareto frontier provided by the multiobjective genetic algorithm after 100 iterations is shown in Figure 2. Each diamond in Figure 2 represents one architecture, i.e., one assignment of instruments to orbits.

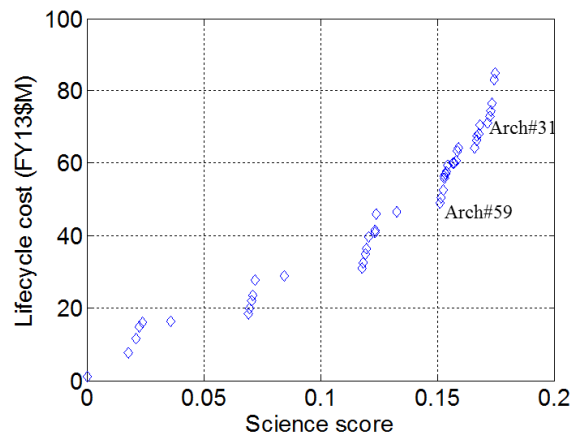


Figure 2: Approximate Pareto frontier after 100 iterations

Table 8: Architectures highlighted in Figure 2

Arch#	Orbit	Instruments
31	SSO-600-SSO-AM	IMAG GPS-RO SPEC MMAS GPS-R
	LEO-600-ISS-NA	not selected
	LEO-400-polar-NA	ERB GPS-RO GRAV
	LEO-400-tropical-NA	not selected
59	SSO-600-SSO-AM	IMAG SPEC MMAS GPS-R
	LEO-600-ISS-NA	not selected
	LEO-400-polar-NA	not selected
	LEO-400-tropical-NA	not selected

Two architectures are highlighted in Figure 2. Their details are provided in Table 8. We start by studying common features in these architectures. Are there any characteristics that appear much more often in Pareto architectures than in dominated architectures? Using the functions of the explanation facility, the following common features were identified:

- (1) 90% of all Pareto architectures leave the 600km ISS orbit empty. Furthermore, the remaining 10% of architectures are located in the highest science region of the Pareto frontier, since as mentioned earlier, this orbit is necessary to achieve the maximum science score. This suggests that the reductions in launch cost from this orbit are not worth unless GPS radio occultation has a very large relative value with respect to other measurements.
- (2) 92% of all Pareto architectures use the 600km SSO orbit. The 8% of architectures that leave this orbit empty all score below 0.03.
- (3) 92% of all Pareto architectures use the millimeter wave sounder. These architectures are found all along the Pareto front. This suggests that this instrument is a cost-effective choice with respect to the Decadal requirements, regardless of the budget.
- (4) 94% of all architectures use the imager, and the remaining 6% of architectures that do not use it are unable to exceed a score of 0.02. This is due to the extremely synergistic nature

of this instrument with several others, as explained in the previous section.

Next, we study the stratified structure of the approximate Pareto frontier. We observe clusters of points relatively separated in both science and cost where it takes a lot of money to obtain marginal increases in science. Simple analysis reveals that neither number of instruments neither number of orbits selected is uniquely driving the clusters, but both of them are strongly correlated with the cluster structure, as shown in Figure 3 and Figure 4. Instead, there are several dominant schemata, such as the one defined by assigning the imager, the GPS-R, the spectrometer and the sounder to the SSO orbit. Architectures on the Pareto front that feature this schema are systematically in the two high cost-high science clusters, as shown in Figure 5. Architectures that have this schema are labeled “Schema ON”, while architectures that do not have it are labeled “Schema OFF”.

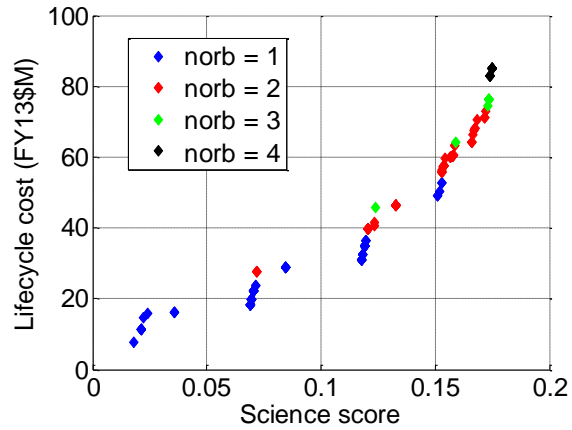


Figure 3: Effect of number of orbits selected on science and cost of architectures on Pareto front

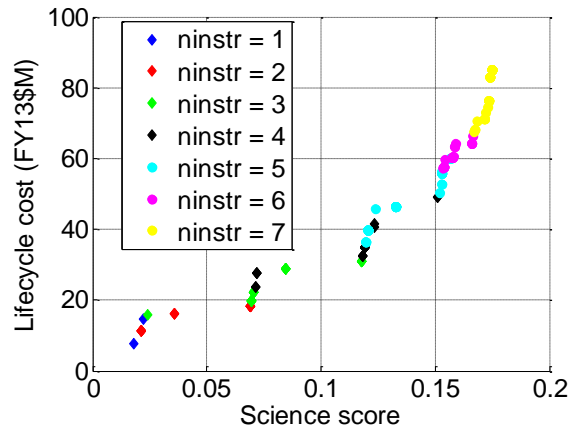


Figure 4: Effect of number of instruments selected on science and cost of architectures on Pareto front

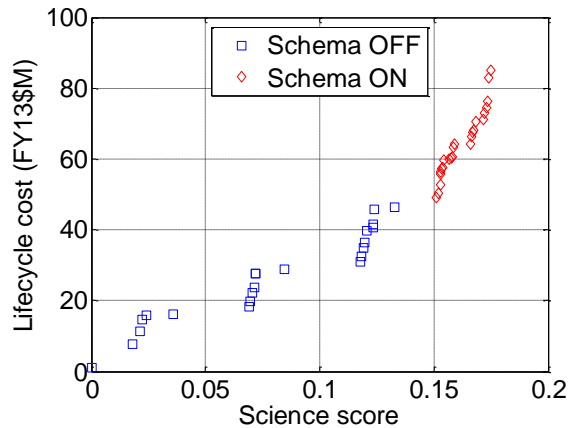


Figure 5: Effect of assigning the IMAG, GPS-R, SPEC, and MMAS to the SSO orbit

Fuzzy scores—The results shown in Figure 2 do not capture the uncertainty that is present in the assessments made for both science and cost. The architectures on the approximate Pareto frontier were evaluated using the fuzzy scoring system presented in the methods section. The results are shown on Figure 6. The error bars represent both the ambiguity and uncertainty present in the cost and science assessments. We observe higher uncertainties for higher values of science and cost. This is expected for the cost estimate, because the uncertainty is modeled as a relative fraction of the expected value, as shown in Table 6. A similar argument can be done for the science assessment, with the caveat that fully satisfied requirements are modeled with crisp scores and therefore do not contribute to increasing the science error bar. The large error bars could indicate that most of the science score comes from providing “some” value or “marginal” value to a relatively high number of requirements, as opposed to fully satisfying a small number of requirements.

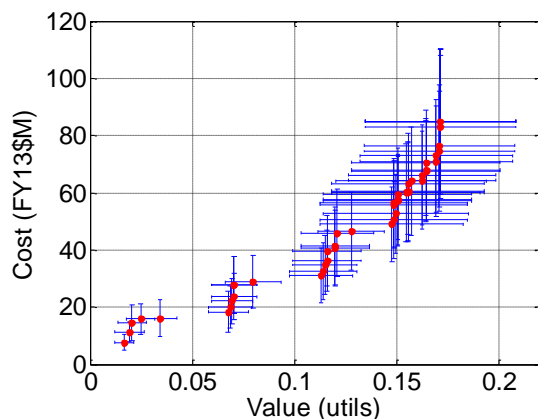


Figure 6: Fuzzy score for Pareto architectures

Selected Architecture—Given the previous considerations, we selected architecture #31 for further studies. The details of this architecture were provided in Table 8. The architecture uses two out of the four orbits, namely the 600km SSO and the 400km polar orbit. It flies exactly one copy of each instrument, except for the GPS-RO which flies on both orbits. The ERB and the GRAV instruments fly in the 400km orbit, with all the other instruments flying in the 600km SSO. This 2-orbit constellation achieves a science score of 0.172, i.e., 87% of the maximum achievable science score, for \$71M, i.e., 70% of the maximum lifecycle cost. Henceforth, architecture #31 will be referred to as EOSSCube.

Mission analysis for EOSSCube

The EOSSCube constellation was selected in the previous section as an interesting compromise between science and cost. In this section, we conduct a preliminary mission analysis for EOSSCube using AGI’s Satellite Tool Kit software, as described in the methods section.

Cubesats in the same orbital plane were separated 15min, forming a train of Cubesats, in order to facilitate cross-registration of their datasets. The mean and total access times of each Cubesat to the ground station were computed. Furthermore, assuming a data rate of 1Mbps (achievable in S-band), it was shown that each Cubesat can download about 1.4Gbit per day. The fraction of sunlight was computed for each Cubesat during the simulation period and found to be between 73-76%. The cumulative distribution function of gap duration is shown for the constellation as a whole in Figure 7, while Figure 8 shows the latitude-longitude dependence. The mean, median, and 90th percentile revisit times are 2.3h, 6.1h, and 12.2h respectively. All these results are summarized in Table 9.

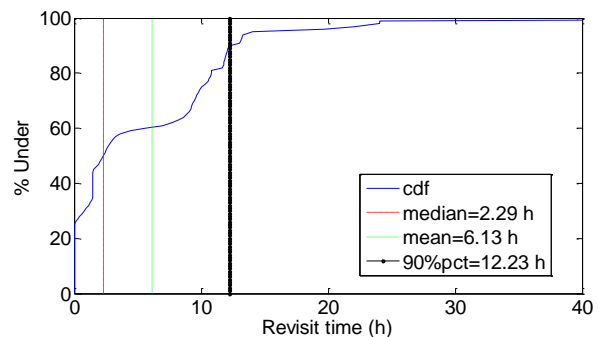


Figure 7: Cumulative distribution function of revisit times for the EOSSCube constellation

Table 9: Results of the preliminary mission analysis for EOSSCube

Parameter	IMAG	SPEC	MMAS	GPS-RO	GPS-R	ERB	GRAV	Constellation
# Cubesat units	2	2	2	1	6	2	1	N/A
Mean access time (min)	12.2	12.2	12.2	12.2	12.2	12.2	12.2	12.2
Total access time (hours)	2.6	2.6	2.6	2.6	2.6	2.6	2.6	2.6
Data volume (Gbit/day)	1.4	1.4	1.4	1.4	1.4	1.4	1.4	1.4
Fraction of sunlight	73%	73%	73%	73%	73%	77%	77%	77%
Median revisit time (h)	N/A	N/A	N/A	N/A	N/A	N/A	N/A	2.3
Mean revisit time (h)	N/A	N/A	N/A	N/A	N/A	N/A	N/A	6.1
90th pct revisit time (h)	N/A	N/A	N/A	N/A	N/A	N/A	N/A	12.2

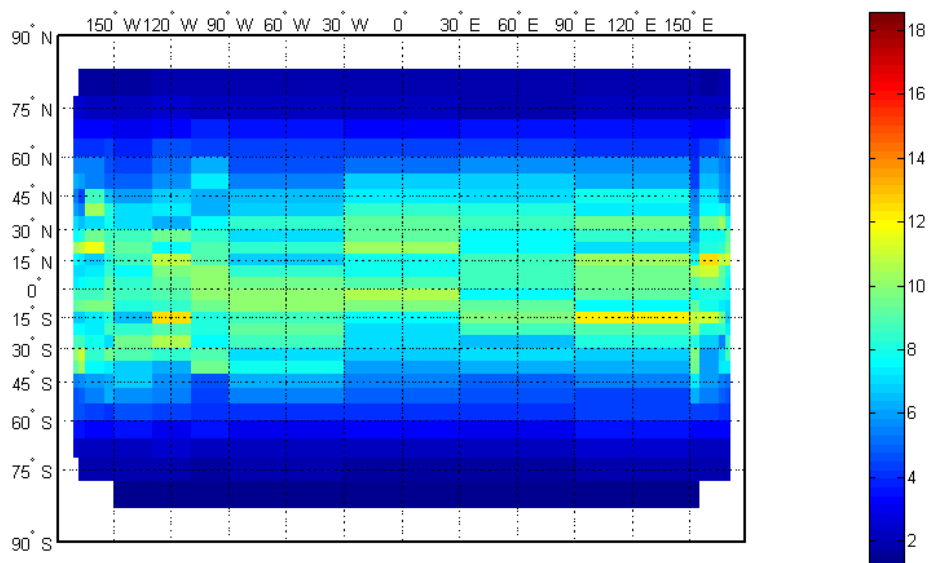


Figure 8: Average revisit time for the entire constellation as a function of latitude and longitude

CONCLUSION

Main results

This article has presented a quantitative analysis to identify Cubesat constellations with potential to satisfy a fraction of the Decadal Survey scientific requirements in a cost-efficient manner. Leveraging previous work, seven candidate instruments, complying with the stringent requirements imposed by Cubesats, were selected for investigation. A tradespace consisting of all assignments of these seven instruments to four orbits was explored.

The main tools used for the analysis are a rule-based expert system for providing relative assessments of the ability of different Cubesat constellations to satisfy Decadal requirements, interval analysis to quantify uncertainty and ambiguity in both science and cost estimations, a multiobjective genetic algorithm to search the science-cost tradespace, and AGI's Satellite Tool Kit software for a preliminary mission analysis on a selected constellation.

An approximate Pareto frontier was found by the genetic algorithm. Architectures in this Pareto frontier tend to use the 600km SSO orbit for most instruments and the 400km polar orbit for the radiation budget and gravity instruments. They tend to leave the 600km 51.6 deg inclination empty. Most of them fly the millimeter wave sounder due to its cost-effective way of providing value to key climate and weather requirements, and the imager due to its highly synergistic nature with several other instruments. A dominant schema was identified that consists in flying the imager, the GPS-R, the spectrometer, and the millimeter wave atmospheric sounder in the SSO orbit. Architectures on the Pareto front featuring this schema systematically appear in the top 10% science region of the tradespace.

A rough analysis of uncertainty and ambiguity in both the cost and science scores shows large error bars in both axis, with larger uncertainties for more costly architectures. Large error bars in the science scores are indicative of the constellation partially satisfying many requirements as opposed to fully satisfying a few requirements.

An architecture was selected for further studies that consists in flying the GPS-RO, the imager, the GPS-R, the spectrometer, and the millimeter wave atmospheric sounder in the SSO orbit, plus the bolometer, the accelerometer, and another GPS-RO in the 400km polar orbit. This architecture, EOSSCube, achieves a score of 0.17 in satisfaction of Decadal requirements while costing around \$70M, a fraction of the cost of any Decadal mission.

Preliminary analysis performed on this architecture shows that its mean revisit time is around 6h, and the 90% percentile is around 12h for the entire constellation. Each Cubesat has around 2h of contacts with a mid-latitude ground station providing around 1.4Gbit of data per day.

Limitations and future work

This work suffers from several limitations. Perhaps the most important one is the large uncertainty surrounding the instrument characteristics, the scientific requirements, and the cost parameters. The science model is largely based on expert knowledge replacing expensive end-to-end simulation models, and therefore its quality is limited by the quality of the knowledge base. More detailed information about the knowledge base can be found in Selva's thesis⁴.

This knowledge base was designed with the Earth Science Decadal Survey in mind, and tested against the NASA Earth Observing System instruments, and it was not originally conceived to maximize its sensitivity to differences between these traditional large instruments and much smaller instruments. Some rules had to be added to it to account for such differences, but more rules of this type are needed in order to increase modeling fidelity. In particular, it is necessary to model simplified error budgets (including both systematic and variable error contributions) for all measurements, as they currently only exist for a few of them.

The propagation of uncertainty and ambiguity in the fuzzy requirements and capabilities was done by simple interval analysis instead of probability distributions due to the lack of data in Cubesat mission costing.

The strong dominance of the SSO orbit in the tradespace analysis might point to possible benefit of including a similar orbit at different altitude to increase sensitivity of the analysis, exploring further possible orbit assignment tradeoffs, e.g. polar and SSO orbits at equally low altitudes.

Finally, the preliminary mission analysis presented in this paper needs to be extended in order to include more precise estimations of mass, power, data rate, and volume budgets for each of the Cubesats. In addition, the possibility of increasing the number of orbital planes for a specific chosen orbit might be studied as a means of decreasing revisit time gaps.

ACKNOWLEDGEMENTS

The authors would like to thank Draper Laboratory and the MIT MISTI program for partially funding this research project.

REFERENCES

- ¹ National Research Council, *Earth Science and Applications from Space: National Imperatives for the Next Decade and Beyond*, Washington DC: The National Academies Press, 2007.
- ² Seher, T., “Campaign-level Science Traceability for Earth Observation System Architecting,” MS Thesis, Dept. of Aeronautics and Astronautics, 2009.
- ³ Selva, D., and Krejci, D., “A Survey and Assessment of the Capabilities of Cubesats for Earth Observation,” *Acta Astronautica*, vol. 74, 2012, pp. 50–68.
- ⁴ Selva, D., “Rule-based system architecting of Earth observation satellite systems,” PhD dissertation, Massachusetts Institute of Technology, ProQuest/UMI, 2012.
- ⁵ Dyrud, L., and Fentzke, J., “GEOScan: a geoscience facility from space,” *SPIE Defense*, ..., 2012, p. 83850V–83850V.
- ⁶ Dyrud, L., Fentzke, J., Bust, G., Erlandson, B., Whitely, S., Bauer, B., Arnold, S., Selva, D., Cahoy, K., Bishop, R., Wiscombe, W., Lorentz, S., Slagowski, S., Gunter, B., and Trenberth, K., “GEOScan: A global, real-time geoscience facility,” *2013 IEEE Aerospace Conference, Big Sky*: 2013, pp. 1–13.
- ⁷ Swab, M., Keefe, K. O., and Skone, S., “Single-frequency Ionospheric Profiles from the CanX-2 nano-satellite,” *ION GNSS*, Nashville,TN: 2012.
- ⁸ Blackwell, W., Allen, G., Galbraith, C., Hancock, T., Leslie, R., Osaretin, I., Retherford, L., Scarito, M., Semisch, C., Shields, M., Silver, M., Toher, D., Wight, K., Miller, D., Cahoy, K., and Erickson, N., “Nanosatellites for earth environmental monitoring: The MicroMAS project,” *2012 12th Specialist Meeting on Microwave Radiometry and Remote Sensing of the Environment (MicroRad)*, Ieee, 2012, pp. 1–4.
- ⁹ Blackwell, W. J., Allen, G., Conrad, S., Galbraith, C., Kingsbury, R., Leslie, R., Mckinley, P., Osaretin, I., Reid, B., Retherford, L., Scarito, M., Semisch, C., Shields, M., Silver, M., Toher, D., Wezalis, R., Wight, K., Cahoy, K., Miller, D. W., Marinar, A., Paek, S. W., Peters, E., Schmidt, F. H., Alvisio, B., Wise, E., Masterson, R., Miranda, D. F., and Erickson, N., “Nanosatellites for Earth Environmental Monitoring: The MicroMAS Project,” *26th Annual AIAA/USU Conference on Small Satellites*, 2012.
- ¹⁰ Kahr, E., O’Keefe, K., and Skone, S., “Optimizing Tracking and Acquisition Capabilities for the CanX-2 Nanosatellite’s COTS GPS Receiver in Orbit,” *Proceedings of the 2010 ION GNSS Technical Meeting*, Nashville,TN: 2010, pp. 21–24.
- ¹¹ Kahr, E., Montenbruck, O., O’Keefe, K., Skone, S., Urbanek, J., Bradbury, L., and Fenton, P., “GPS tracking on a nanosatellite—the CanX-2 flight experience,” *8th International ESA conference on Guidance, Navigation & Control Systems*, 2011.
- ¹² Camps, A., Rodriguez-Alvarez, N., Bosch-Lluis, X., Marchan, J. F., Ramos-Perez, I., Segarra, M., Sagues, L., Tarrago, D., Cunado, O., Vilaseca, R., Tomas, A., Mas, J., and Guillamon, J., “PAU in SeoSAT: A proposed hybrid L-band microwave radiometer/GPS reflectometer to improve Sea Surface Salinity estimates from space,” *Proceedings of the 2008 Conference on Microwave Radiometry and Remote Sensing of the Environment*, Ieee, 2008.
- ¹³ Minelli, G., Ricco, A., Beasley, C., and Hines, J., “O/OREOS nanosatellite: A multi-payload technology demonstration,” *24th Annual AIAA/USU Conference on Small Satellites*, 2010.
- ¹⁴ Kitts, C., Rasay, M., Bica, L., Mas, I., and Neumann, M., “Initial On-Orbit Engineering Results from the O/OREOS Nanosatellite,” *25th Annual AIAA/USU Conference on Small Satellites*, 2011.
- ¹⁵ Bramall, N. E., Quinn, R., Mattioda, A., Bryson, K., Chittenden, J. D., Cook, A., Taylor, C., Minelli, G., Ehrenfreund, P., Ricco, A. J., Squires, D., Santos, O., Friedericks, C., Landis, D., Jones, N. C., Salama, F., Allamandola, L. J., and Hoffmann, S. V., “The development of the Space Environment Viability of Organics (SEVO) experiment aboard the Organism/Organic Exposure to Orbital Stresses (O/OREOS) satellite,” *Planetary and Space Science*, vol. 60, Jan. 2012, pp. 121–130.
- ¹⁶ Dyrud, L. P., Fentzke, J. T., Bust, G., Erlandson, B., Bauer, B., Rogers, A. Q.,

- Wiscombe, W., Murphy, S., Bishop, R., Cahoy, K., and Fish, C., "GEOScan: A GEOScience Facility From Space," *26th Annual AIAA/USU Conference on Small Satellites*, 2012.
- 17 Selva, D., and Crawley, E., "VASSAR: Value Assessment of System Architectures using Rules," *Aerospace Conference, 2013 IEEE*, Big Sky: IEEE, 2013.
- 18 Zadeh, L. A., "Fuzzy Sets," *Information and Control*, vol. 8, Jan. 1965, pp. 338–353.
- 19 Woellert, K., Ehrenfreund, P., Ricco, A. J., and Hertzfeld, H., "Cubesats: Cost-effective science and technology platforms for emerging and developing nations," *Advances in Space Research*, vol. 47, Feb. 2011, pp. 663–684.
- 20 Baker, D. N., and Worden, S. P., "The Large Benefits of Small-Satellite Missions," *Eos, Transactions American Geophysical Union*, vol. 89, 2008, p. 301.
- 21 Kitts, C., Ronzano, K., Rasay, R., Mas, I., and Hines, J., "The GeneSat-1 Biological Nanosatellite Mission," *IEEE Aerospace and Electronic Systems Magazine*.
- 22 Diaz-Aguado, M. F., Minnelli, G., Ghassemieh, S., Beasley, C., and Schooley, A., "O/OREOS and PharmaSat – Thermal Lessons Learned on Small Class D Spacecraft," *4th Conference on Environmental Systems*, 2011.
- 23 Deb, K., Pratap, A., Agarwal, S., and Meyarivan, T., "A fast and elitist multiobjective genetic algorithm: NSGA-II," *IEEE Transactions on Evolutionary Computation*, vol. 6, Apr. 2002, pp. 182–197.